Varying boreal forest response to Arctic environmental change at the Firth River, Alaska

Laia Andreu-Hayles[1,2]**, Rosanne D'Arrigo**[1]**, Kevin J Anchukaitis**[1]**, Pieter S A Beck**[3]**, David Frank**[4,5] **and Scott Goetz**[3]

[1] Tree-Ring Laboratory, Lamont-Doherty Earth Observatory of Columbia University, 61 Route 9W, Palisades, NY 10964, USA
[2] Institut Català de Ciències del Clima (IC3), C/ Dr Trueta 203, 08005 Barcelona, Catalonia, Spain
[3] Woods Hole Research Center, 149 Woods Hole Road, Falmouth, MA, USA
[4] Swiss Federal Research Institute WSL, Birmensdorf, Switzerland
[5] Oeschger Centre for Climate Change Research, University of Bern, Switzerland

E-mail: lah@ldeo.columbia.edu

Abstract

The response of boreal forests to anthropogenic climate change remains uncertain, with potentially significant impacts for the global carbon cycle, albedo, canopy evapotranspiration and feedbacks into further climate change. Here, we focus on tree-ring data from the Firth River site at treeline in northeastern Alaska, in a tundra–forest transition region where pronounced warming has already occurred. Both tree-ring width (TRW) and maximum latewood density (MXD) chronologies were developed to identify the nature of tree growth and density responses to climatic and environmental changes in white spruce (*Picea glauca*), a dominant Arctic treeline species. Good agreement was found between the interannual fluctuations in the TRW chronology and summer temperatures from 1901 to 1950, whereas no significant relationships were found from 1951 to 2001, supporting evidence of significant divergence between TRW and summer temperature in the second half of the 20th century. In contrast to this unstable climatic response in the TRW record, the high frequency July–August temperature signal in the MXD series seems reasonably stable through the 20th century. Wider and denser rings were more frequent during the 20th century, particularly after 1950, than in previous centuries. Finally, comparison between the tree-ring proxies and a satellite-derived vegetation index suggests that TRW and MXD correlate with vegetation productivity at the landscape level at different times of the growing season.

1. Introduction

In the Arctic, temperatures have increased during the last century at nearly double the global average rate (ACIA 2005, Trenberth *et al* 2007) and substantial biotic and abiotic impacts in the Arctic environment have already been documented (ACIA 2005, Hinzman *et al* 2005). These changes can feed back to the climate system through a variety

of processes including changes in albedo, emissions from permafrost thawing, and shifts in the fire regime, among other factors, potentially attenuating or accelerating Arctic climate change (ACIA 2005, Serreze *et al* 2009). Boreal forests might help mitigate global warming through increased carbon sequestration, but at the same time their low albedo may provide a positive climate feedback to warming (Bonan 2008). The sensitivity of Arctic terrestrial ecosystems to warming and changes in seasonality is likely to be highly complex, involving shifts in the timing and dynamics of multiple climatological and ecological factors that can significantly impact the ecotone between tundra and boreal forests.

Satellite-derived indices of photosynthetic activity such as the normalized difference vegetation index (NDVI) are commonly used to document changes in northern forest growth patterns (Myneni *et al* 1997, Beck *et al* 2006, 2007). In recent decades, opposing vegetation productivity trends have been observed between boreal forests, which show decreasing productivity, and tundra, which shows increasing productivity. This pattern is discernable at northern circumpolar high latitudes (Bunn and Goetz 2006, Goetz *et al* 2007), across North America (Goetz *et al* 2005), and particularly in Alaska (Verbyla 2008, Beck *et al* 2011). Thus, remote sensing observations show 'browning' of vegetation in interior Alaska, which transitions to 'greening' of vegetation in the Alaskan tundra, with an intervening region of relatively little trend in photosynthetic activity. Growth patterns at this forest–tundra ecotone appear to be driven by a variety of environmental factors and have not yet been well documented (Lloyd and Bunn 2007, Berner *et al* 2011). Tree-ring samples collected at the Arctic treeline provide a unique record for understanding growth dynamics at this ecotone, and complement the patterns of large-scale vegetation dynamics obtained through satellite data.

In the latter part of the 20th century, a weakening of the previously observed relationship between tree rings and local to larger-scale temperatures has been reported in some forests at higher northern latitudes (Briffa *et al* 1998, Driscoll *et al* 2005, Wilmking *et al* 2005, Wilson *et al* 2007, D'Arrigo *et al* 2009). This phenomenon has become known as the 'divergence problem' and has potentially far-reaching implications for the global carbon cycle, forest growth patterns and paleoclimatic reconstructions (D'Arrigo *et al* 2008). The detection (Esper and Frank 2009) and processes (D'Arrigo *et al* 2008) underlying the observed differences in temperature sensitivity between and within forest stands are still under debate. Possible mechanistic causes for 'divergence' include drought stress and other nonlinear physiological responses to recent warming, a poorly understood sensitivity of tree growth to temperature extremes rather than means, snowmelt delay, seasonality changes, or a reduction in available solar radiation for large-scale vegetation growth during the last decades (D'Arrigo *et al* 2008).

In northwestern America, the divergence phenomenon is widespread in tree-ring width (TRW) records (Jacoby and D'Arrigo 1995, Barber *et al* 2000, Lloyd and Fastie 2002, D'Arrigo *et al* 2005), but some forest stands still maintain a positive growth response to temperature (Driscoll *et al* 2005,

Wilmking *et al* 2005). Some studies have also identified divergence in maximum latewood density (MXD) data (Jacoby and D'Arrigo 1995, Briffa *et al* 1998, Wilson and Luckman 2003, D'Arrigo *et al* 2004). Others instead report stability between temperature and density records (Barber *et al* 2000, D'Arrigo *et al* 2009), allowing reconstruction of past summer temperatures from MXD proxies (Davi *et al* 2003, Anchukaitis *et al* 2011).

In comparison to TRW, MXD is generally less sensitive to site ecology, site temperature/elevation, species under investigation and previous year climate, making it a more robust indicator of climate conditions toward the cold thermal treeline (Frank and Esper 2005). Latewood cells, formed at the end of the growing season, have smaller diameters and thicker walls resulting in a higher xylem density than the larger and thinner earlywood cells, formed during the main course of the growing season. Compared to earlywood, latewood is less dependent on resources stored during the previous growth year. TRW integrates growth resulting from cell division and enlargement over the entire length of the growing season, while the MXD metric is more linked to a cell maturation phase that includes thickening and lignification of the secondary cell walls in the latewood tracheids. Thus, the influence of environmental factors upon these two tree-ring parameters can vary (Kirdyanov *et al* 2007).

Our study site within the Firth River watershed is a white spruce forest stand located at the Arctic latitudinal treeline of northeastern Alaska, where tree growth is expected to be primarily limited by temperature. We studied this site to assess changes in tree growth at the tundra–boreal forest ecotone. More precisely, two millennial length tree-ring chronologies based on TRW and MXD, respectively, were developed to (1) assess the stability of the climatic signal registered in both tree-ring parameters for the 20th century, (2) identify changes in tree growth and density, and (3) establish a linkage between the tree-ring proxies and vegetation indices produced from satellite remote sensing data.

2. Data and methods

2.1. Study site and tree-ring chronologies

Living and subfossil wood samples of white spruce (*Picea glauca*) were collected from the Firth River area of the Alaskan National Wildlife Refuge (ANWR) in 2002 at latitudinal treeline (68.78N, 142.35W). Trees were growing in scattered groves over hilly slopes in an open valley at the Firth River watershed. The subfossil wood was collected from both standing and toppled dead trees. Collectively, these samples have yielded one of the very few millennial length tree-ring records presently available for northern Alaska (figure 1).

The TRW chronology is composed of 232 radii from 111 trees (30 living and 81 from subfossil wood) and spans from 1067 to 2002 AD. It was generated at the Tree-Ring Laboratory of the Lamont-Doherty Earth Observatory using standard dendrochronological methods (Stokes and Smiley 1968, Fritts 1976). These TRW data were included previously as part of a broader network of circumpolar northern chronologies used
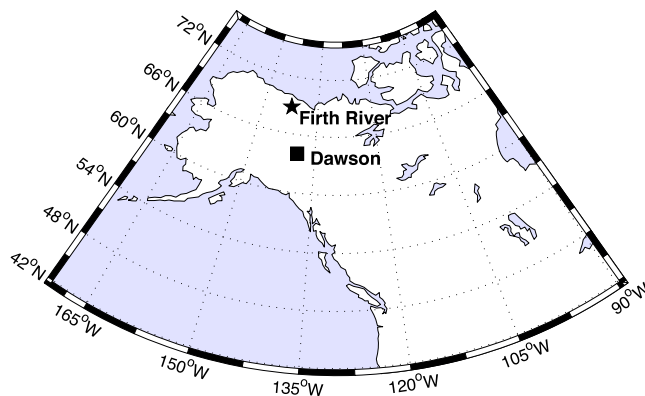
Figure 1. Map of northwestern America showing the study site at the Firth River in Alaska and the meteorological station located in Dawson, Canada.

to reconstruct extratropical northern hemisphere temperatures (D'Arrigo *et al* 2006). The MXD measurements were performed using a Dendro 2003 (Walesch) x-ray densitometer system (Eschbach *et al* 1995) at the Swiss Federal Research Institute WSL in Birmensdorf, Switzerland. The MXD chronology, spanning from 1073 to 2002 AD, is based on 246 measurement time series from 30 living and 74 subfossil trees that were also used for building the TRW chronology.

2.2. Standardization methods

Both TRW and MXD raw individual tree-ring series were standardized using the program ARSTAN (Cook 1985). Different detrending methods were applied: a spline function (Cook and Peters 1981) with a 50% frequency response of 140 yr (SP140); negative exponential or negative linear regression (NEXP); and regional curve standardization (RCS) (Cook and Kairiukstis 1990) after stabilizing the variance with a power transform (PT) technique (Cook and Peters 1997, Helama *et al* 2004). The adequacy of the data-adaptive curves (SP140/NEXP) and RCS to preserve low frequency variance has been questioned due to the 'trend distortion' problem (Melvin and Briffa 2008, Briffa and Melvin 2011). Thus, the signal free (SF) standardization method (Melvin and Briffa 2008), which has been suggested as a solution to this problem, was also tested. Individual detrended series were combined into master site chronologies using the biweight robust mean (Cook and Kairiukstis 1990). 'Residual' chronologies, series without autocorrelation, reflect prewhitening using autoregressive modeling on the individual width or density series. Prewhitening was used to remove the *persistence* or dependence of past values in current year data. The order of the autoregressive model was selected based on the first-minimum Akaike Information Criteria implemented in the program ARSTAN (Cook 1985). The 'Expressed Population Signal' (EPS) statistic, a measure of the strength of the common climate signal in the tree-ring proxies, remains consistently above the commonly applied quality threshold of 0.85 (Wigley *et al* 1984) after approximately 1300 AD and 1250 AD for TRW and MXD chronologies, respectively.

2.3. Meteorological and remote sensing data

Both meteorological station and gridded climate data were compared to the Firth tree-ring chronologies. We used monthly mean, maximum and minimum temperature data observed at Dawson (Vincent and Gullett 1999), Yukon Territory, the longest meteorological records (since 1897) in the vicinity of the Firth River about 540 km away (figure 1). We explored spatial field correlations between the tree-ring data and several monthly gridded data sets: mean temperature and precipitation from CRU TS 2.1 0.5° from 1901 to 2002 (Mitchell and Jones 2005); mean temperature anomalies from the GISTEMP 2° product smoothed at 1200 km from 1880 to 2010 generated by the Goddard Institute for Spaces Studies (GISS) (Hansen *et al* 2010) and provided by NOAA/OAR/ESRL PSD, Boulder, Colorado, USA (www.esrl.noaa.gov/psd/NOAA); and the Palmer drought severity index (PDSI) 2.5° from 1870 to 2005 (Dai *et al* 2004).

To provide landscape-wide estimates of vegetation productivity for comparison with the tree-ring proxies, we used the normalized difference vegetation index (NDVI) data set produced by NASA's Global Inventory Modeling and Mapping Studies (GIMMS-NDVI version 3G) from Advanced Very High Resolution Radiometer data. The data span July 1981–2008 and are produced twice monthly at a 0.084° spatial resolution (Pinzon and Tucker 2010).

2.4. Data analyses

The associations between climate and tree-ring variables were assessed using correlation analysis. To compare correlation coefficients they were converted using a Fisher transformation so that quasi-normality with variance $1/(n-3)$ could be assumed. Two-tailed tests were performed, with the null hypothesis being that there was no difference between distributions. We determined the statistical significance of any epochal change in correlation coefficients following Snedecor and Cochran (1989).

We also used raw TRW and MXD data to assess tree growth and wood density variations during the 20th century to avoid possible artifacts due to dendrochronological standardization methods, similar to the approach used by Salzer *et al* (2009) with bristlecone pine. Here, we removed the first 150 yr and rings older than 300 yr from all the series in order to mitigate age/size trends and to compare throughout time tree rings from trees within the same age range (figures S4a and S5a available at stacks.iop.org/ERL/6/045503/mmedia). The frequency distributions of the TRW and MXD values, as well as the corresponding empirical cumulative distribution function (CDF), were calculated for different time periods. The nonparametric Kolmogorov–Smirnov (KS) test was then used to determine the significance of the differences observed between the empirical CDFs.

The agreement between the remotely sensed vegetation index and tree-ring proxies was assessed by extracting the spatially averaged NDVI time series over a 3 × 3 window of grid cells coinciding with the Firth River site. Applying the 3 × 3 window buffered any geospatial inaccuracies in the GIMMS-NDVI data. The NDVI time series was then
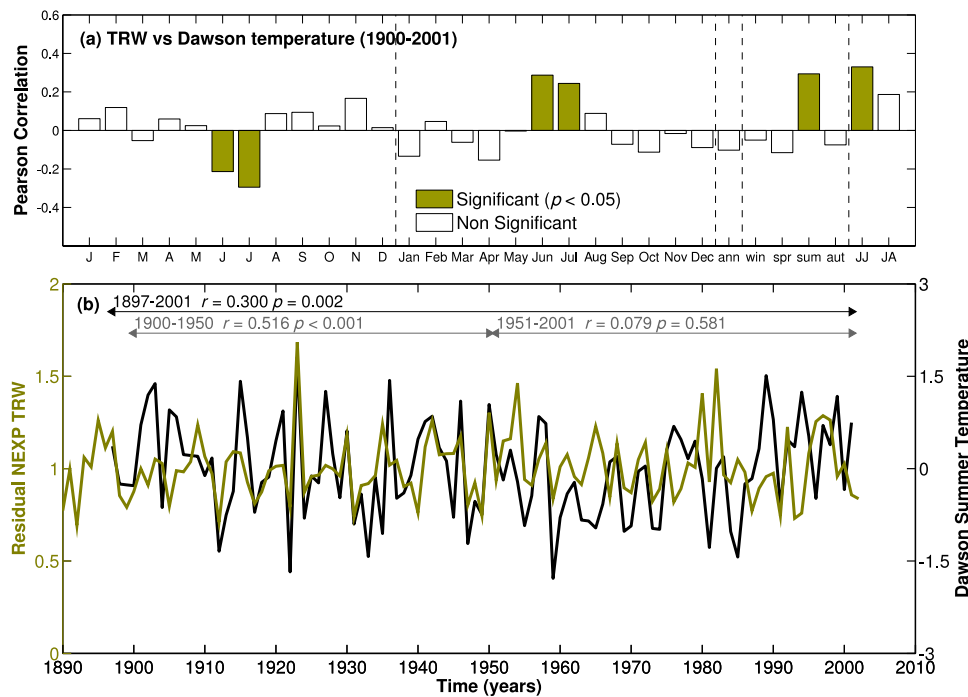
Figure 2. (a) Pearson correlation between the residual NEXP tree-ring width (TRW) chronology and mean monthly temperature anomalies from Dawson for the previous year (uppercase) and for the current year (lowercase). Correlations using annual, seasonal, June–July (JJ) and July–August (JA) periods are also displayed for the current year. (b) Residual NEXP TRW chronology and Dawson summer temperature anomalies versus time. Correlations (r) and p-value (p) between these two series are indicated for different time periods.

resampled to monthly resolution at fortnightly intervals and compared to the tree-ring chronologies. Correlations were calculated between yearly TRW or MXD and NDVI values using the Pearson product-moment correlation coefficient and Kendall's τ.

3. Results

3.1. Stability of the high frequency temperature signal in the tree-ring proxies

As we focus herein on the high frequency domain, i.e. the year-to-year relationship between climate and tree rings, only the prewhitened residual TRW and MXD chronologies were used for comparison with the meteorological data that were converted to anomalies after removing the trends. Since nearly identical results were obtained using the SP140, NEXP or RCSPT residual chronologies, only results using the NEXP are shown. Autoregressive models of orders 4 and 2 were used to obtain the NEXP residual chronology for TRW and MXD, respectively. The residual TRW chronology shows significant ($p < 0.05$) positive Pearson's correlation coefficients for June and July current year Dawson mean temperatures during the 20th century, as well as significant negative correlations for the same months of the previous year (figure 2(a)). The correlation with summer temperature anomalies was significant for the first, but not for the second, half of the 20th century (figure 2(b)). Pearson's correlation between the residual MXD chronology and May, July and August

current year Dawson mean temperatures were positive and significant for the 1900–2001 period, whereas no significant relationships were found with temperatures from the previous year (figure 3(a)). Figure 3(b) depicts that July–August temperature anomalies were significantly related to the MXD record throughout the 20th century, showing similar correlation values for both halves of the century. Correlations with maximum temperatures were slightly lower than with mean temperatures but produced almost identical results. When using minimum temperatures correlations were even much lower showing a similar pattern for TRW, but not for MXD that displayed an unstable relationship with July–August throughout time (results not shown). All the analyses were repeated using prewhitened meteorological series obtaining the same main results than using the detrended data (results not shown).

Figure 4 compares the correlations between the tree-ring proxies and May to August current year temperatures for both periods: 1900–50 and 1951–2001. For TRW, the declines in correlations with June and summer temperatures were significant at 95% confidence level, while the declines in correlations with August, June–July and July–August were significant at 90% confidence level. For MXD, the only significant change ($p < 0.05$) was the decrease in the correlation with June temperature, while all the other changes in correlation between both periods were statistically indistinguishable.

Spatial field correlations obtained using the CRU TS 2.1 or GISTEMP data sets were very similar, thus only GISTEMP results are shown. Field correlations between
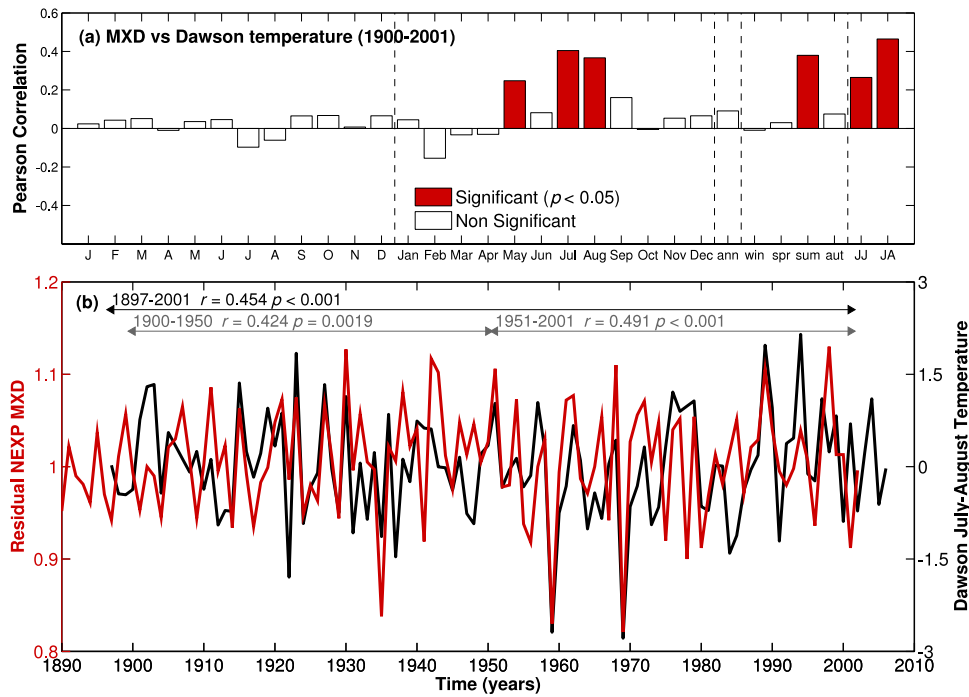
Figure 3. (a) Pearson correlation between the residual NEXP maximum latewood density (MXD) tree-ring chronology and mean monthly temperature anomalies from Dawson for the previous year (uppercase) and for the current year (lowercase). Correlations using annual, seasonal, June–July (JJ) and July–August (JA) periods are also displayed for the current year. (b) Residual NEXP MXD chronology and Dawson July–August temperature anomalies versus time. Correlations (r) and p-value (p) between these two series are indicated for different time periods.
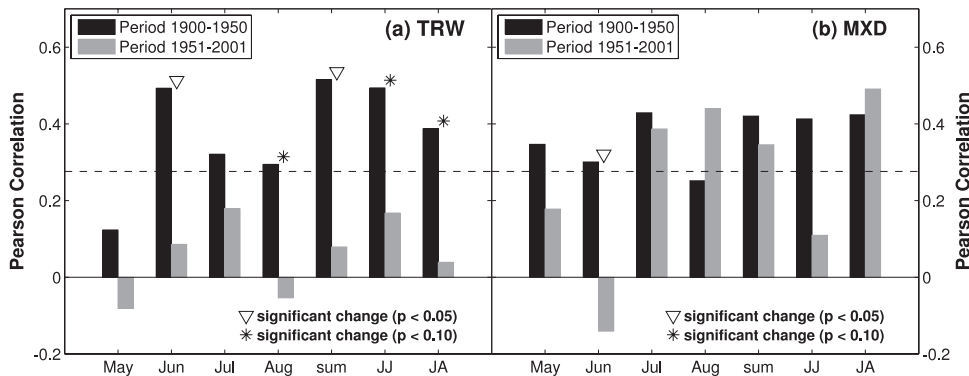

Figure 4. Pearson correlations between the residual tree-ring width (TRW) chronology (a) and the residual maximum latewood density (MXD) tree-ring chronology (b) versus May to August, summer, June–July (JJ) and July–August (JA) mean temperature anomalies from Dawson for two periods: 1900–50 (black bars) and 1951–2001 (gray bars). White arrows and asterisks indicate that the difference between the correlations of the two periods is significant at 95% and at 90% confidence level, respectively. Dashed horizontal lines indicate the 95% significance level of correlation.

the TRW chronology (figure S1 available at stacks.iop.org/ ERL/6/045503/mmedia) and the MXD chronology (figure S2 available at stacks.iop.org/ERL/6/045503/mmedia) versus May to August gridded mean temperatures confirm the results obtained with Dawson local station data for a larger spatial scale. A complete absence of statistically significant summer temperature signals during the second half of the 20th century was found for TRW, whereas the July–August temperature signal remained for MXD during both studied periods. No coherent patterns were found when comparing the tree-ring chronologies with precipitation or PDSI monthly gridded data (results not shown).

Considering tree-ring data before prewhitening, TRW series have high autocorrelations and significant partial autocorrelations for 4 years (figure S3 available at stacks.iop. org/ERL/6/045503/mmedia), while lagged relationships are almost negligible for MXD series. Thus, the MXD parameter is less dependent on conditions in preceding years than TRW.

3.2. Variations in tree growth and maximum density

To assess tree growth and density variations, the raw tree-ring data were used after eliminating the first 150 yr from all the series and all rings older than 300 yr. Hence,
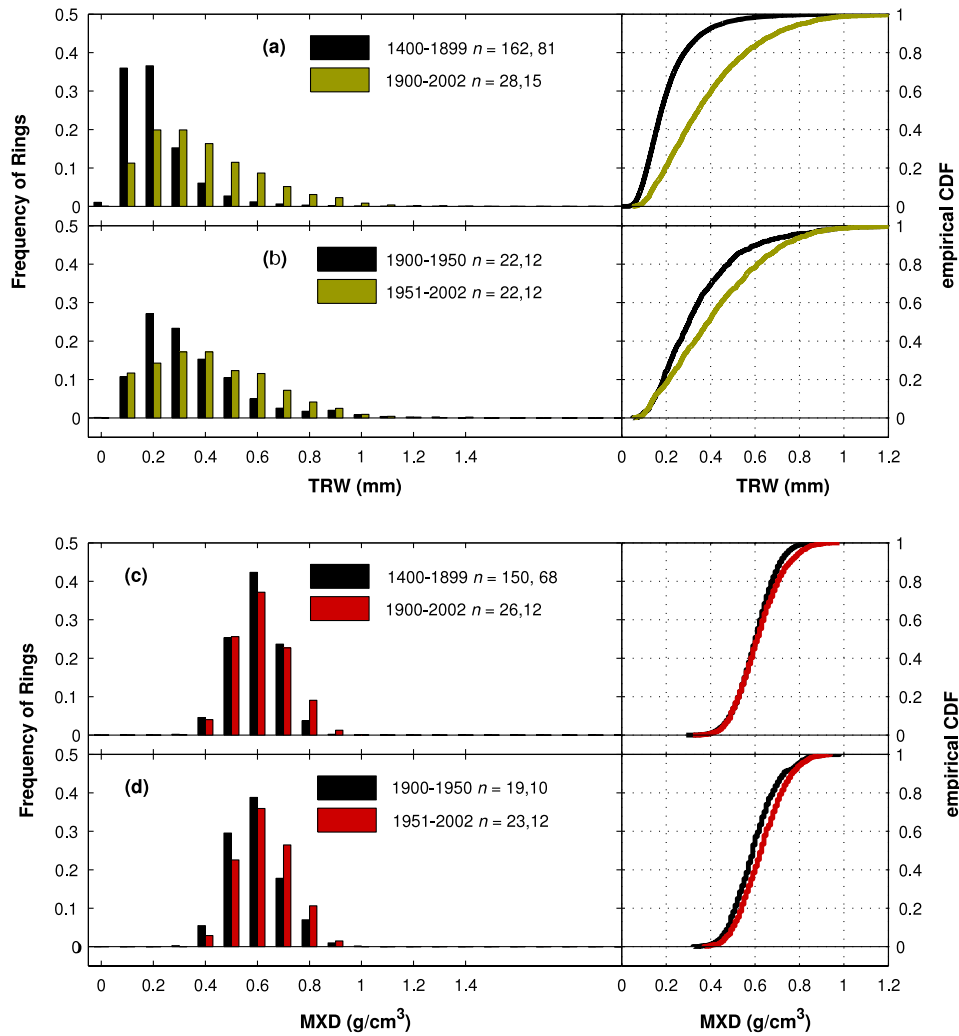
Figure 5. Raw TRW and MXD data after removing from all the series the first 150 yr and rings older than 300 yr. *n* indicates the number of radii followed by the number of trees for each group. (a) Left: TRW frequencies from 1900–2002 in comparison to the frequencies prior to 1900 since 1400. (b) Left: TRW frequencies from 1900–50 versus 1951–2002. (c) Left: MXD frequencies from 1900–2002 in comparison to the frequencies prior to 1900 since 1400. (d) Left: MXD frequencies from 1900–50 versus 1951–2002. Right panels: empirical cumulative distribution function (CDF) for the same groups of TRW and MXD data.

only information in this age range (i.e. 150–300 yr) was considered. Figures S4a and S5a (available at stacks.iop. org/ERL/6/045503/mmedia) illustrate the mean raw TRW and MXD chronologies, respectively, before and after the removal of rings. The TRW and MXD frequency histograms and CDFs for different time periods were compared starting from 1400 AD (figure 5). After 1400 AD, an acceptable number of samples still remained after the removal of the selected rings: 23 radii from 13 trees for raw TRW data and 27 radii from 10 trees for raw MXD data, and in both cases sample size increases up to 2002. A higher frequency of wider rings was observed from 1900 to 2002 in comparison with the period before 1900 (figure 5(a)), as well as during the second half of the 20th century relative to the first half (figure 5(b)). The empirical CDF (figures 5(a), (b), right panels) and the KS test (table S1a available at stacks.iop.org/ ERL/6/045503/mmedia) of both comparisons demonstrated that TRW distributions were significantly different, showing a

detectable shift toward wider rings after 1900, and even wider after 1950.

Rings show higher MXD values from 1900 to 2002 than before 1900 (figure 5(c)). In the 20th century (figure 5(d)), MXD values were higher during the second half than during the first half. The empirical CDF (figures 5(c), (d), right panels) and the KS test (table S1b available at stacks.iop.org/ ERL/6/045503/mmedia) indicate that the MXD distribution show significantly denser rings during the 20th century in comparison with previous centuries, and even denser after 1950.

Table S1 (available at stacks.iop.org/ERL/6/045503/ mmedia) also shows the statistics obtained for the longest available time periods (1217 and 1223 AD for TRW and MXD, respectively), considering only living trees or using all the available data without removing any rings. Overall, all tests lead to the same conclusions except when using all raw MXD data that do not show significant differences between the first and the second half of the 20th century.
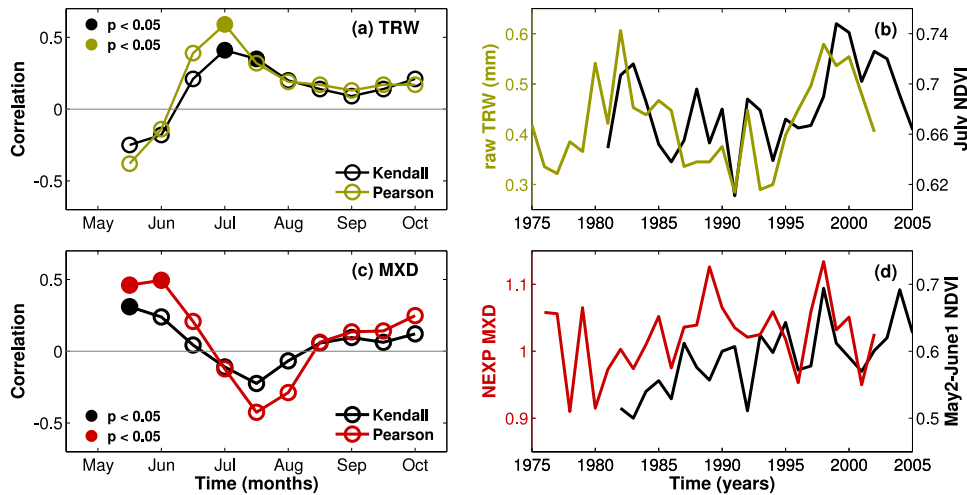
Figure 6. Tree-ring chronologies and monthly NDVI data at fortnightly intervals from May to October. (a) Pearson and Kendall correlations from 1982–2002 between the mean raw 'selected' TRW chronology, obtained after removing the first 150 yr and rings older than 300 yr from all the series, and NDVI data. (b) The mean raw selected TRW chronology and July NDVI versus time. (c) Pearson and Kendall correlations from 1982–2002 between the standard NEXP MXD chronology and NDVI data. (d) The standard NEXP MXD chronology and NDVI data from the second half of May and the first half of June (May2–June1) versus time.

Significant upward trends were found in mean raw TRW and MXD chronologies since 1850 AD, the beginning of industrialization, and since 1901 AD (figures S4 and S5 available at stacks.iop.org/ERL/6/045503/mmedia lower panels). However, no significant trends were detected since 1950 AD and 1981 AD (the starting date of NDVI data), except for the chronology built using all raw TRW series, which is likely influenced by age-related trends in the youngest living trees.

3.3. Comparisons between tree-ring data and NDVI

Significant linkages were found between the tree-ring proxies and NDVI (figure 6). Table S2 (available at stacks.iop.org/ERL/6/045503/mmedia) summarizes Pearson and Kendall correlations obtained between monthly NDVI data at fortnightly intervals and the TRW chronologies standardized using different methods (see section 2.2 for details). Table S3 (available at stacks.iop.org/ERL/6/045503/mmedia) shows the same for the MXD chronologies. Overall, the strongest positive correlations between the TRW chronologies and NDVI were found in July (figures 6(a) and (b)).

The MXD chronologies (table S3 available at stacks.iop.org/ERL/6/045503/mmedia) correlated strongest with the NDVI from the second half of May (May2) to the first half of June (June1). Additionally, negative correlations were detected with late summer NDVI data. Figure 6(c) shows results obtained by plotting the correlations between the standard NEXP MXD chronology and NDVI data, whereas figure 6(d) shows this chronology together with May2–June1 NDVI data versus time. Although the observed patterns seem consistent, these exploratory results should be interpreted with caution because there were relatively few degrees of freedom (i.e. short time intervals) in the correlation analyses.

4. Discussion and conclusions

Varying tree growth responses to climate change were studied at the Firth River white spruce stand in Alaska. Although the most relevant and significant environmental factor influencing the two tree-ring proxies was temperature, the stability of the climatic signal was diverse. While the MXD chronology maintains a significant positive relationship with summer mean temperatures throughout the 20th century, the TRW chronology only shows a positive relationship during the first half of the century, an indication of the 'divergence' phenomenon previously reported (D'Arrigo *et al* 2008). Our findings demonstrate a loss of sensitivity of tree growth to temperature in the high frequency domain. Thus, the observed divergence at this northern latitudinal treeline is not merely an artifact of detrending methods applied during the tree-ring standardization process (Melvin and Briffa 2008). Forests where 'divergence' is detected may have reached a threshold beyond which tree growth is no longer positively influenced by summer temperature. This could be linked to the unusually rapid warming of the late 20th century due to recent anthropogenic change (ACIA 2005, Trenberth *et al* 2007), as well as potentially greater moisture stress due to an increase in evapotranspiration demand (Angert *et al* 2005, Lotsch *et al* 2005, Bunn and Goetz 2006, Beck *et al* 2011). Data from the Bonanza Creek Long Term Ecological Research in central Alaska indicate increases in the summer vapor pressure deficit from 1988 to 2008 (Beck *et al* 2011).

Nevertheless, whereas temperature-induced drought stress has been suggested as a potential cause of the white spruce growth decline observed in interior Alaska (Barber *et al* 2000, McGuire *et al* 2010) and at some warmer sites below treeline, at colder sites located at alpine or Arctic treelines no detectable growth decreases have been reported (Lloyd and Fastie 2002). Here, we do not detect any growth reduction at the northern Alaskan treeline. Rather, our results indicate wider rings

during the 20th century and even wider rings after 1950. Although no positive tree growth trends were detected for the most recent decades, in agreement with some remote sensing results at the tundra–boreal ecotone (Verbyla 2008, Beck *et al* 2011), the several centuries long term perspective provided by the dendrochronological approach indicates a longer term growth enhancement. Therefore, our results based on tree-ring samples collected *in situ* suggest an increase in forest productivity at this forest–tundra transition zone.

The MXD proxy contains a noteworthy stable July–August temperature signal, although a complete mechanistic understanding of the causes remains unknown. MXD series show much lower autocorrelations than TRW series and do not show any significant relationships with temperatures from the previous year, indicating that MXD is controlled primarily by current year conditions, potentially providing more precise environmental information (i.e. climatic signal) for a given year. MXD is related to cell differentiation processes, such as thickening or lignification of the secondary cell walls in latewood tracheids, which occur when growth rates decline at the end of the summer season. This generally happens in the July–August period, which is when we found significant MXD–temperature relationships. Aside from the temperature effect on xylogenesis (Körner 1998, Rossi *et al* 2007), the photoperiod may be regulating the timing of tree-ring formation rates: the highest growth rates come about the period of maximum day length and after this peak growth rates begin to decrease, providing sufficient time for finishing cell differentiation before the winter (Rossi *et al* 2006). Therefore, the earlywood/latewood transition may be mainly controlled by the photoperiod length giving stability to the starting date of latewood formation in contrast to a greater variability in the onset of the growing season which may be more dependent on temperature thresholds (Körner 1998, Körner and Paulsen 2004). Therefore, TRW may be more influenced than MXD by changes in phenological patterns linked to ongoing warming (Menzel and Fabian 1999) or variations in snowfall and timing of snowmelt (Vaganov *et al* 1999).

Considering that divergence between TRW proxies and summer temperatures has implications in paleoclimatic reconstructions, MXD records may in some cases be a more reliable proxy at the northern sites where temperature no longer seems to be the primary factor controlling tree growth. Other tree-ring proxies, such as stable isotopes, should be explored since the climatic signal reflected by these proxies arise from different physiological mechanisms, such as stomatal regulation due to changes in moisture availability.

The significant linkages documented between our tree-ring ground-based measurements and NDVI data provide support to the landscape-wide representation of boreal vegetation growth through satellite vegetation indices. The reasonable agreement between summer NDVI and TRW, which integrates annual radial growth for the entire growing season, suggests that NDVI reflects carbon uptake by means of canopy activity. Similarly, several studies have significantly related TRW with summer NDVI in the taiga (Kaufmann *et al* 2004, Lopatin *et al* 2006, Kaufmann *et al* 2008, Berner *et al* 2011) corroborating the relevance of the physiological status of

the canopy during summer in forest productivity. In addition to D'Arrigo *et al* (2000), our investigation is among just a few comparing NDVI and MXD data. While the negative association between MXD and summer NDVI may link a decrease in canopy activity with lower growth rates and thus the onset of MXD (Rossi *et al* 2006), the positive relationship with late spring/early summer NDVI would indicate some influence of timing and/or vigor of early growing season phases on the cell differentiation processes. Future research using an extended tree-ring network would be desirable in order to confirm the patterns observed in our case study at the Firth River.

Acknowledgments

References

ACIA 2005 *Arctic Climate Impact Assessment* (Cambridge: Cambridge University Press)

Anchukaitis K J *et al* 2011 Summer temperatures in northwestern North America during the last nine centuries *J. Clim.* under revision

Angert A *et al* 2005 Drier summers cancel out the CO_2 uptake enhancement induced by warmer springs *Proc. Natl Acad. Sci. USA* **102** 10823–7

Barber V A, Juday G P and Finney B P 2000 Reduced growth of Alaskan white spruce in the twientieth century from temperature-induced drought stress *Nature* **405** 668–73

Beck P S A, Atzberger C, Høgda K A, Johansen B and Skidmore A K 2006 Improved monitoring of vegetation dynamics at very high latitudes: a new method using MODIS NDVI *Remote Sens. Environ.* **100** 321–34

Beck P S A, Jönsson P, Høgda K-A, Karlsen S R, Eklundh L and Skidmore A K 2007 A ground-validated NDVI dataset for monitoring vegetation dynamics and mapping phenology in Fennoscandia and the Kola peninsula *Int. J. Remote Sens.* **28** 4311–30

Beck P S A *et al* 2011 Changes in forest productivity across Alaska consistent with biome shift *Ecol. Lett.* **14** 373–9

Berner L T, Beck P S A, Bunn A G, Lloyd A H and Goetz S J 2011 High-latitude tree growth and satellite vegetation indices: correlations and trends in Russia and Canada (1982–2008) *J. Geophys. Res.* **116** G01015

Bonan G B 2008 Forests and climate change: forcings, feedbacks, and the climate benefits of forests *Science* **320** 1444–9

Briffa K R and Melvin T M 2011 A closer look at regional curve standardization of tree-ring records: justification of the need, a warning of some pitfalls, and suggested improvements in its application *Dendroclimatology: Progress and Prospects* (*Developments in Paleoenvironmental Research* vol 11) ed M K Hughes, T W Swetnam and H F Diaz (Berlin: Springer) pp 113–46

Briffa K R, Schweingruber F H, Jones P D, Osborn T J, Shiyatov S G and Vaganov E A 1998 Reduced sensitivity of recent tree-growth to temperature at high northern latitudes *Nature* **391** 678–82

Bunn A G and Goetz S J 2006 Trends in circumpolar satellite observed gross photosynthesis from 1982–2003: the role of cover type and vegetation density *Earth Interact.* **10** 1–19

Cook E R 1985 A time series analysis approach to tree-ring standardization *PhD Thesis* University of Arizona, Tucson, AZ, USA

Cook E R and Kairiukstis L (ed) 1990 *Methods of Dendrochronology: Applications in the Environmental Sciences* (Dordrecht: Kluwer) p 394

Cook E R and Peters K 1981 The smoothing spline: a new approach to standardizing forest interior tree-ring width series for dendroclimatic studies *Tree-Ring Bull.* **41** 45–53

Cook E R and Peters K 1997 Calculating unbiased tree-ring indices for the study of climatic and environmental change *Holocene* **7** 359–68

D'Arrigo R, Mashig E, Frank D, Jacoby G and Wilson R 2004 Reconstructed warm season temperatures for Nome, Seward Peninsula, Alaska *Geophys. Res. Lett.* **31** L09202

D'Arrigo R, Mashig E, Frank D, Wilson R and Jacoby G 2005 Temperature variability over the past millennium inferred from Northwestern Alaska tree rings *Clim. Dyn.* **24** 227–36

D'Arrigo R, Wilson R and Jacoby G 2006 On the long-term context for late twentieth century warming *J. Geophys. Res.* **111** D03103

D'Arrigo R, Wilson R, Liepert B and Cherubini P 2008 On the 'Divergence problem' in northern forests: a review of the tree-ring evidence and possible causes *Glob. Planet. Change* **60** 289–305

D'Arrigo R *et al* 2009 Tree growth and inferred temperature variability at the North American Arctic treeline *Glob. Planet. Change* **65** 71–82

D'Arrigo R D, Malmstrom C M, Jacoby G C, Los S O and Bunker D E 2000 Correlation between maximum latewood density of annual tree rings and NDVI based estimates of forest productivity *Int. J. Remote Sens.* **21** 2329–36

Dai A, Trenberth K E and Qian T 2004 A global data set of Palmer drought severity index for 1870–2002: relationship with soil moisture and effects of surface warming *J. Hydrometeorol.* **5** 1117–30

Davi N K, Jacoby G C and Wiles G C 2003 Boreal temperature variability inferred from maximum latewood density and tree-ring width data, Wrangell Mountain region Alaska *Quat. Res.* **60** 252–62

Driscoll W W, Wiles G C, D'Arrigo R D and Wilmking M 2005 Divergent tree growth response to recent climatic warming, Lake Clark National Park and Preserve, Alaska *Geophys. Res. Lett.* **32** L20703

Eschbach W, Nogler P, Schär E and Schweingruber F 1995 Technical advances in the radiodensitometrical determination of wood density *Dendrochronologia* **13** 155–68

Esper J and Frank D 2009 Divergence pitfalls in tree-ring research *Clim. Change* **94** 261–6

Frank D and Esper J 2005 Characterization and climate response patterns of a high-elevation, multi-species tree-ring network in the European Alps *Dendrochronologia* **22** 107–21

Fritts H 1976 *Tree Rings and Climate* (New York: Academic) p 433

Goetz S J, Bunn A G, Fiske G J and Houghton R A 2005 Satellite-observed photosynthetic trends across boreal North America associated with climate and fire disturbance *Proc. Natl Acad. Sci. USA* **102** 13521–5

Goetz S J, Mack M C, Gurney K R, Randerson J T and Houghton R A 2007 Ecosystem responses to recent climate change and fire disturbance at northern high latitudes observations and model results contrasting northern Eurasia and North America *Environ. Res. Lett.* **2** 045031

Hansen J, Ruedy R, Sato M and Lo K 2010 Global surface temperature change *Rev. Geophys.* **48** RG4004

Helama S, Lindholm M, Timonen M and Eronen M 2004 Detection of climate signal in dendrochronological data analysis: a comparison of tree-ring standardization methods *Theor. Appl. Climatol.* **79** 239–54

Hinzman L *et al* 2005 Evidence and implications of recent climate change in Northern Alaska and other Arctic regions *Clim. Change* **72** 251–98

Jacoby G C and D'Arrigo R D 1995 Tree-ring width and density evidence of climatic and potential forest change in Alaska *Glob. Biogeochem. Cycles* **9** 227–34

Kaufmann R K, D'Arrigo R D, Laskowski C, Myneni R B, Zhou L and Davi N K 2004 The effect of growing season and summer greenness on northern forests *Geophys. Res. Lett.* **31** L09205

Kaufmann R K, D'Arrigo R D, Paletta L F, Tian H Q, Jolly W M and Myneni R B 2008 Identifying climatic controls on ring width: the timing of correlations between tree rings and NDVI *Earth Interact.* **12** 14

Kirdyanov A, Vaganov E and Hughes M 2007 Separating the climatic signal from tree-ring width and maximum latewood density records *Trees-Struct. Funct.* **21** 37–44

Körner C 1998 A re-assessment of high elevation treeline positions and their explanation *Oecologia* **115** 445–59

Körner C and Paulsen J 2004 A world-wide study of high altitude treeline temperatures *J. Biogeogr.* **31** 713–32

Lloyd A H and Bunn A G 2007 Responses of the circumpolar boreal forest to 20th century climate variability *Environ. Res. Lett.* **2** 045013

Lloyd A H and Fastie C L 2002 Spatial and temporal variability in the growth and climate response of treeline trees in Alaska *Clim. Change* **52** 481–509

Lopatin E, Kolstrom T and Spiecker H 2006 Determination of forest growth trends in Komi Republic (northwestern Russia): combination of tree-ring analysis and remote sensing data *Boreal Environ. Res.* **11** 341–53

Lotsch A, Friedl M A, Anderson B T and Tucker C J 2005 Response of terrestrial ecosystems to recent northern hemispheric drought *Geophys. Res. Lett.* **32** L06705

McGuire A D, Ruess R W, Lloyd A, Yarie J, Clein J S and Juday G P 2010 Vulnerability of white spruce tree growth in interior Alaska in response to climate variability: dendrochronological, demographic, and experimental perspectives *Can. J. Forest Res.* **40** 1197–209

Melvin T M and Briffa K R 2008 A 'signal-free' approach to dendroclimatic standardisation *Dendrochronologia* **26** 71–86

Menzel A and Fabian P 1999 Growing season extended in Europe *Nature* **397** 659

Mitchell T D and Jones P D 2005 An improved method of constructing a database of monthly climate observations and associated high-resolution grids *Int. J. Climatol.* **25** 693–712

Myneni R B, Keeling C D, Tucker C J, Asrar G and Nemani R R 1997 Increased plant growth in the northern high latitudes from 1981 to 1991 *Nature* **386** 698–702

Pinzon J E and Tucker C J 2010 GIMMS 3g NDVI set and global NDVI trends *Second Yamal Land-Cover Land-Use Change Workshop Arctic Centre (Rovaniemi, March)* (www.geobotany. uaf.edu/yamal/rovMtg/ptText.php?queryID=168)

Rossi S, Deslauriers A, Anfodillo T and Carraro V 2007 Evidence of threshold temperatures for xylogenesis in conifers at high altitudes *Oecologia* **152** 1–12

Rossi S, Deslauriers A, Anfodillo T, Morin H, Saracino A, Motta R and Borghetti M 2006 Conifers in cold environments synchronize maximum growth rate of tree-ring formation with day length *New Phytol.* **170** 301–10

Salzer M W, Hughes M K, Bunn A G and Kipfmueller K F 2009 Recent unprecedented tree-ring growth in bristlecone pine at the highest elevations and possible causes *Proc. Natl Acad. Sci.* **106** 20348–53

Serreze M C, Barrett A P, Stroeve J C, Kindig D N and Holland M M 2009 The emergence of surface-based Arctic amplification *Cryosphere* **3** 11–9

Snedecor G W and Cochran W G 1989 *Statistical Methods* 8th edn (Ames, IA: Iowa State University Press)

Stokes M and Smiley T 1968 *An Introduction to Tree-Ring Dating* (Chicago, IL: University of Chicago Press) p 73

Trenberth K E *et al* 2007 Observations: surface and atmospheric climate change *Climate Change 2007: The Physical Science Basis. Contribution of Working Group I to the Fourth Assessment Report of the Intergovernmental Panel on Climate Change* ed S Solomon, D Qin, M Manning, Z Chen, M Marquis, K B Averyt, M Tignor and H L Miller (Cambridge: Cambridge University Press)

Vaganov E A, Hughes M K, Kirdyanov A V, Schweingruber F H and Silkin P P 1999 Influence of snowfall and melt timing on tree growth in subarctic Eurasia *Nature* **400** 149–51

Verbyla D 2008 The greening and browning of Alaska based on 1982–2003 satellite data *Glob. Ecol. Biogeogr.* **17** 547–55

Vincent L A and Gullett D W 1999 Canadian historical and homogeneous temperature datasets for climate change analyses *Int. J. Climatol.* **19** 1375–88

Wigley T M L, Briffa K R and Jones P D 1984 On the average value of correlated time series, with applications in dendroclimatoly and hydrometeorology *J. Clim. Appl. Meteorol.* **23** 201–13

Wilmking M, D'Arrigo R, Jacoby G C and Juday G P 2005 Increased temperature sensitivity and divergent growth trends in circumpolar boreal forests *Geophys. Res. Lett.* **32** L15715

Wilson R J S and Luckman B H 2003 Dendroclimatic reconstruction of maximum summer temperatures from upper treeline sites in Interior British Columbia, Canada *Holocene* **13** 851–61

Wilson R *et al* 2007 A matter of divergence: tracking recent warming at hemispheric scales using tree ring data *J. Geophys. Res.—Atmos.* **112** D17103